

## One-loop Higgs boson production at the Linear Collider within the general two-Higgs-doublet model: $e^+e^-$ versus $\gamma\gamma$

J. SOLÀ<sup>(1)</sup> and D. LÓPEZ-VAL<sup>(2)</sup>

<sup>(1)</sup> *High Energy Physics Group, Dept. ECM, and Institut de Ciències del Cosmos  
Univ. de Barcelona - Av. Diagonal 647, E-08028 Barcelona, Catalonia, Spain*

<sup>(2)</sup> *Institut für Theoretische Physik, Universität Heidelberg  
Philosophenweg 16, D-69120 Heidelberg, Germany*

(ricevuto il 20 Luglio 2011; pubblicato online il 6 Ottobre 2011)

**Summary.** — We present an updated overview on the phenomenology of one-loop Higgs boson production at Linear Colliders within the general Two-Higgs-Doublet Model (2HDM). First we report on the Higgs boson pair production, and associated Higgs-Z boson production, at  $\mathcal{O}(\alpha_{ew}^3)$  from  $e^+e^-$  collisions. These channels furnish cross-sections in the range of 10–100 fb for  $\sqrt{s} = 0.5$  TeV and exhibit potentially large radiative corrections ( $|\delta_r| \sim 50\%$ ), whose origin can be traced back to the genuine enhancement capabilities of the triple Higgs boson self-interactions. Next we consider the loop-induced production of a single Higgs boson from direct  $\gamma\gamma$  scattering. We single out sizable departures from the expected  $\gamma\gamma \rightarrow h$  rates in the Standard Model, which are again correlated to trademark dynamical features of the 2HDM—namely the balance of the non-standard Higgs/gauge, Higgs/fermion and Higgs self-interactions, which leads to sizable (destructive) interference effects. This pattern of quantum effects is unmatched in the MSSM, and could hence provide distinctive footprints of non-supersymmetric Higgs boson physics. Both calculations are revisited within a common, brought-to-date framework and include, in particular, the most stringent bounds from unitarity and flavor physics.

PACS 12.15.-y – Electroweak interactions.

PACS 12.60.Fr – Extensions of electroweak Higgs sector.

PACS 12.15.Lk – Electroweak radiative corrections.

### 1. – Introduction and computational framework

The quest for experimental evidence of the Higgs boson is actively underway at the Tevatron and the LHC [1]. Nonetheless, a complete understanding of the Electroweak Symmetry Breaking conundrum will not only demand to discover the Higgs boson, but also to precisely measure its mass, quantum numbers and interactions to the other particles. A Linear Collider (linac, hereafter), such as the ILC or the CLIC, would be the most natural facility to carry this endeavor to completion [2] and, perhaps most

significantly, to disentangle the Standard Model (SM) Higgs mechanism from its many potential extensions.

The Two-Higgs-Doublet Model (2HDM) [3] constitutes a singularly simple, and yet phenomenologically very rich example of the latter. The absence of tree-level flavor changing neutral currents determines the Higgs/fermion Yukawa couplings and leads to the canonical type-I and type-II realizations of the 2HDM [3]. Moreover, it effectively accounts for the low-energy Higgs sector of some more fundamental theories, such as the Minimal Supersymmetric Standard Model (MSSM) [4]. The 2HDM can be fully specified in terms of the masses of the physical Higgs particles; the parameter  $\tan\beta$  (the ratio  $\langle H_2^0 \rangle / \langle H_1^0 \rangle$  of the two VEV's giving masses to the up- and down-like quarks); the mixing angle  $\alpha$  between the two  $CP$ -even states; and, finally, of one genuine Higgs boson self-coupling, usually denoted as  $\lambda_5$ . We refer the reader to ref. [5] for full details on the model setup, our notation, definitions and various constraints.

While in the context of the MSSM we expect a panoply of Yukawa, and Yukawa-like, couplings of various kinds (including squark interactions with the Higgs bosons), whose phenomenological implications have been exploited in the past in a variety of important processes (see, *e.g.*, [6]), in the case of the general 2HDM we count on alternative mechanisms. Above all, the Higgs self-interactions are perhaps the very trademark structure of the 2HDM. Unlike their MSSM counterparts, the triple ( $3h$ ) and quartic ( $4h$ ) Higgs self-couplings are not restricted by the gauge symmetry, and so they can be potentially enhanced. In favorable circumstances, these enhancements can translate into highly distinctive signatures of a non-standard, non-supersymmetric Higgs sector. Dedicated literature on the topic includes, *e.g.*, the tree-level studies on triple Higgs boson production,  $e^+e^- \rightarrow 3h$  [7], inclusive Higgs-pair production through gauge boson fusion,  $e^+e^- \rightarrow V^*V^* \rightarrow 2h + X$  [8], and the double Higgs-strahlung channels  $e^+e^- \rightarrow hhZ^0$  [9]. Also significant are the loop-induced single Higgs production,  $\gamma\gamma \rightarrow h$  [10] and the double Higgs channels  $\gamma\gamma \rightarrow 2h$  [11]. They have both been considered in the framework of a photon-photon collider, alongside with the complementary radiative decay mode  $h \rightarrow \gamma\gamma$  [12]. Finally, the impact of these  $3h$  self-couplings (see, *e.g.*, Table II of [5]) has been quantified at the level of radiative corrections through the detailed one-loop analysis of the pairwise production of both charged [13] and neutral [5] Higgs boson pairs, as well as upon the study of the associated Higgs-strahlung channels  $e^+e^- \rightarrow h^0Z^0, H^0Z^0$  at the quantum level [13,14]<sup>(1)</sup>. The effective enhancing power of the Higgs self-interactions is subdued, in practice, by a number of experimental constraints and theoretical consistency conditions: perturbativity, unitarity and vacuum stability, as well as from the EW precision data, the low-energy flavor-physics inputs and the Higgs mass regions ruled out by the LEP and Tevatron direct searches—*cf.*, *e.g.*, ref. [17-20].

## 2. – One-loop Higgs boson production from $e^+e^-$

In the following we present a full-fledged one-loop analysis of the  $CP$ -conserving pair production of neutral Higgs bosons ( $e^+e^- \rightarrow 2h = h^0A^0/H^0A^0$ ), alongside with the associated Higgs/ $Z^0$  boson (*Higgs-strahlung*) channels within the 2HDM. On top of the complete set of  $\mathcal{O}(\alpha_{ew}^3)$  corrections, we also retain the leading  $\mathcal{O}(\alpha_{ew}^4)$  terms which stem from the (squared of the)  $\mathcal{O}(\lambda_{3h}^2)$  Higgs-mediated contributions. Renormalization of the

---

<sup>(1)</sup> For related work in the context of radiative corrections in Higgs production processes, see, *e.g.*, [15]. Phenomenological prospects for the LHC have been addressed in [16].

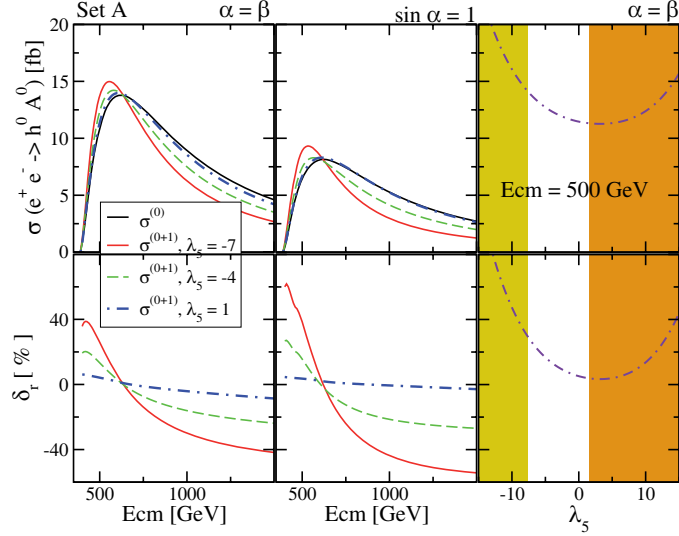


Fig. 1. – (Colour on-line) Total cross-section  $\sigma(h^0 A^0)$  (in fb) and relative one-loop correction  $\delta_r$  (in %) for Set A of Higgs boson masses. Left and central panels display these quantities as a function of  $\sqrt{s}$  (indicated as Ecm). The results are shown within three different values of  $\lambda_5$  at fixed  $\tan\beta = 1.2$  (compatible with the lower  $\tan\beta$  bound from  $B_d^0 - \bar{B}_d^0$  data [18]) and for the representative choices  $\alpha = \beta$  (maximum tree-level coupling) and  $\alpha = \pi/2$  (fermiophobic limit of  $h^0$  for type-I 2HDM). In the right panel we show their evolution in terms of  $\lambda_5$  at  $\sqrt{s} = 500$  GeV. The shaded areas on the left (respectively, right) are excluded by unitarity (respectively, vacuum stability).

SM fields and coupling constants is performed in the conventional on-shell scheme in the Feynman gauge [21]. A dedicated extension of the on-shell scheme is worked out for the 2HDM Higgs sector in [5]. Phenomenological constraints are implemented by interfacing our numerical codes with the packages *2HDMCalc* [22], *SuperISO* [18] and *HiggsBounds* [23], altogether with several complementary in-house routines. As for the algebraic calculation and numerical evaluation of the cross-sections under study, we have employed the standard computational software *FeynArts*, *FormCalc* and *LoopTools* [24]. Representative choices for the Higgs boson spectrum are sorted out in two sets as follows:

	$M_{h^0}$ (GeV)	$M_{H^0}$ (GeV)	$M_{A^0}$ (GeV)	$M_{H^\pm}$ (GeV)
Set A	130	200	260	300
Set B	115	165	100	105

We point out that both sets satisfy the custodial symmetry bound  $|\delta\rho| < 10^{-3}$  [5].

Our interest here is basically threefold, namely: i) to seek for regions within the 2HDM parameter space sourcing large quantum corrections, which we shall quantify through the ratio  $\delta_r \equiv \sigma^{(1)}/\sigma^{(0)}$ , where  $\sigma^{(1)} = \sigma - \sigma^{(0)}$  is the one-loop correction with respect to the tree-level value; ii) to evaluate their impact on the overall 2h and hZ production rates (cf. figs. 1-3); and iii) to correlate these effects to the strength of the  $3h$  self-couplings.

Worth noticing is that the Higgs/gauge boson couplings ( $hZZ$ ,  $hAZ$ ) driving these processes at the leading-order are anchored by the gauge symmetry, and hence take the same form in both the 2HDM and the MSSM. Genuine differences between both models

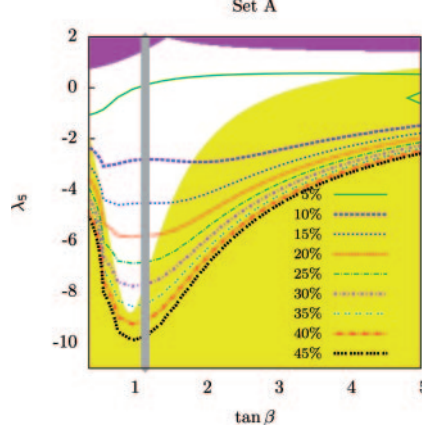


Fig. 2. – (Colour on-line) Radiative corrections  $\delta_r$  (%) to the total cross-section  $\sigma(h^0 A^0)$  as a function of  $\tan\beta$  and  $\lambda_5$ , for Set A of Higgs boson masses,  $\alpha = \beta$  and  $\sqrt{s} = 0.5$  TeV. The shaded areas in the top (respectively, bottom) account for the vacuum stability [20] (respectively, unitarity [19]) conditions, while the vertical grey band depicts the lower limit  $\tan\beta \simeq 1.18$  ensuing from  $B_d^0 - \bar{B}_d^0$  [18].

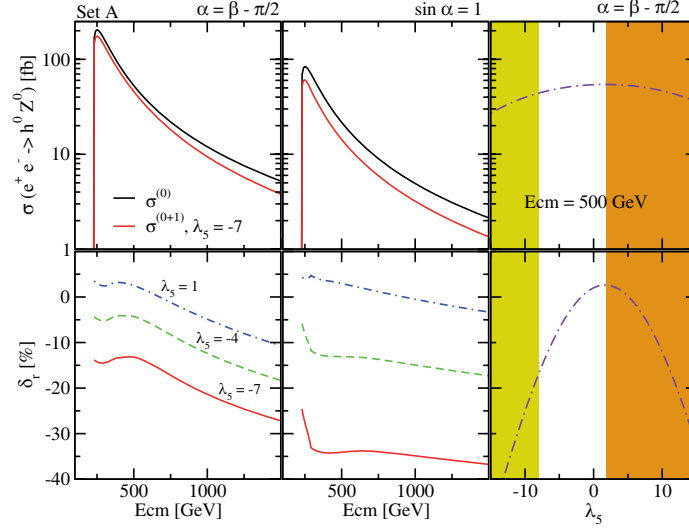


Fig. 3. – (Colour on-line) Total cross-section  $\sigma(h^0 Z^0)$  (in fb) and relative one-loop correction  $\delta_r$  (in %) for Set A of Higgs boson masses. Left and central panels display these quantities as a function of  $\sqrt{s}$ , for three different values of  $\lambda_5$ ,  $\tan\beta = 1.2$  and for the representative choices  $\alpha = \beta - \pi/2$  and  $\alpha = \pi/2$ . In the right panel we show their evolution in terms of  $\lambda_5$  at  $\sqrt{s} = 500$  GeV. The shaded areas on the left (respectively, right) are excluded by unitarity (respectively, vacuum stability).

should thus be probed through the study of quantum effects – among which the enhanced  $3h$  self-interactions of the 2HDM could rubber-stamp a very distinctive imprint.

Let us concentrate on Set A of Higgs boson masses for the analysis of this section. This set is possible in both type-I and type-II 2HDM's [3]. (Set B, characterized by lighter Higgs masses, will be used for  $\gamma\gamma$  physics in the next section; it is only allowed for type-I models.) The cross-section for the particular channel  $h^0 A^0$  as a function of the center-of-mass energy  $\sqrt{s}$  (Ecm), displayed for a few values of  $\lambda_5$ , and also as a function of  $\lambda_5$  at fixed  $\sqrt{s}$ , is shown in fig. 1, together with the relative quantum correction  $\delta_r$ . The rightmost panel of this figure illustrates the expected  $\sigma \sim \sigma_0 + \mathcal{O}(\lambda_5^2) + \mathcal{O}(\lambda_5)$  behavior triggered by the triple Higgs boson self-interactions [5]. The cross-sections at one-loop lie in the approximate range of 2–15 fb for  $\sqrt{s} = 0.5$  TeV—rendering  $10^3$ – $10^4$  events per  $500 \text{ fb}^{-1}$  of integrated luminosity. The corresponding quantum effects are large and positive for  $\sqrt{s}$  around the nominal startup energy of the ILC, *i.e.* 0.5 TeV, but become rapidly negative for  $\sqrt{s} \gtrsim 0.6$  TeV and stay highly so in the entire  $\mathcal{O}(1)$  TeV regime. This sign flip in combination with the behavior of the quantum effects on the Higgs-strahlung processes (see below) gives an important experimental handle on the physics of Higgs production in the 2HDM. Although we have used Set A for the analysis, the behavior of  $\delta_r$  turns out to be fairly independent of the details of the Higgs mass spectrum, the particular type of 2HDM and the specific channel under analysis ( $h^0 A^0$  or  $H^0 A^0$ ).

A dedicated study of the quantum effects  $\delta_r$  as a function of  $\tan\beta$  and  $\lambda_5$  is explored in fig. 2, at fixed  $\sqrt{s} = 500$  GeV. We can also appreciate in it the interplay with the unitarity bounds (lower area, in yellow) and the vacuum stability conditions (upper area, in purple). Notice that the former disallows simultaneously large values of  $\tan\beta$  and  $\lambda_5$ , whereas the latter enforces  $\lambda_5 \lesssim 1$ , but mainly in the negative range:  $-10 < \lambda_5 < 0$ . The largest attainable quantum effects ( $|\delta_r| \sim 20$ – $60\%$ ) are localized in a valley-shaped region centered at  $\tan\beta \gtrsim 1$  deep in the allowed  $\lambda_5 < 0$  range (cf. fig. 2). Here a subset of  $3h$  self-couplings becomes substantially augmented—their strength growing with  $\sim |\lambda_5|$ —and stands as a preeminent source of radiative corrections via Higgs-boson mediated one-loop corrections to the  $hA^0 Z^0$  vertex. As a result this interaction vertex, which is purely gauge at the tree-level, can be drastically modified at the one-loop order. There is, however, the rigid lower bound  $\tan\beta \gtrsim 1$  from  $B_d^0 - \bar{B}_d^0$  oscillations [18] (see the vertical grey band in fig. 2), which further restricts the valley-shaped region and finally leaves less than half of its original allowance for the largest possible quantum effects. In addition to the pairwise production of Higgs bosons we find the more traditional Higgs-strahlung channels ( $e^+e^- \rightarrow h^0 Z^0, H^0 Z^0$ ) [14], *i.e.* the 2HDM analog(s) of the so-called Bjorken process in the SM [25]. As reported in fig. 3 (left and central panels), we obtain typical cross-sections in the ballpark of  $\sigma(h^0 Z^0) \sim \mathcal{O}(10$ – $100)$  fb, which may undergo substantial (and mostly negative) radiative corrections up to order  $\delta_r \sim -50\%$  for large  $3h$  self-coupling enhancements—these being preferably realized for  $\tan\beta = \mathcal{O}(1)$  and  $|\lambda_5| \sim \mathcal{O}(10)$ . The trademark negative sign of the leading quantum effects can be tracked down to the dominance of the finite wave-function corrections to the external Higgs boson fields, this being the only contribution at one loop which retains a quadratic dependence on  $\lambda_{3h}$  ( $\sim \lambda_5$  for  $|\lambda_5| > 1$ ). The rightmost panel of fig. 3 nicely illustrates the characteristic  $\sigma \sim \sigma_0 - \mathcal{O}(\lambda_5^2) + \mathcal{O}(\lambda_5)$  behavior induced by the triple Higgs boson self-interactions, which in this case produce dominant (and negative) quantum effects of  $\mathcal{O}(\lambda_5^2)$  from the wave function renormalization as long as the regime  $|\lambda_5| > 1$  is well attained [14]. As hinted before, the correlation of large negative quantum effects on the Higgs-strahlung channels with the presence of significant positive (for  $\sqrt{s} \lesssim 500$  GeV) and large negative (for  $\sqrt{s} > 600$  GeV) quantum effects on the double Higgs production

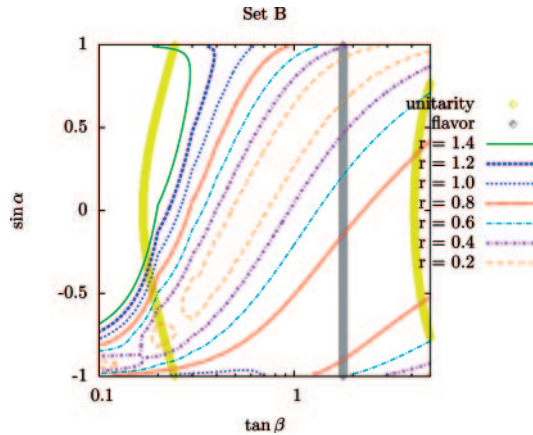


Fig. 4. – (Colour on-line) Effective  $\gamma\gamma h^0$  coupling strength in the 2HDM normalized to the SM,  $r \equiv g_{\gamma\gamma h^0}/g_{\gamma\gamma H}^{\text{SM}}$ , in terms of  $\sin\alpha$  and  $\tan\beta$ . The yellow strips signal the lower and upper bounds stemming from unitarity, while the grey vertical band ensues from the  $\bar{B}_d^0 - B_d^0$  constraints at the  $3\sigma$  level.

channels could eventually lead to a robust quantum signature of (non-supersymmetric) 2HDM physics in a Linear Collider.

### 3. – One-loop Higgs boson production from $\gamma\gamma$

Direct  $\gamma\gamma$  collisions may be realized through Compton backscattering of high energetic laser pulses off the original  $e^+e^-$  linac beams [26]. This alternative running mode opens up a plethora of complementary experimental strategies for a Linear Collider. In particular, it may provide a pristine insight into the loop-induced  $\gamma\gamma h$  coupling—and so to the underlying structure of the Higgs sector. This effective interaction ensues from an interplay of gauge boson, fermion and charged scalar one-loop contributions [27]. In the 2HDM the charged Higgs-mediated effects, which are directly sensitive to the  $3h$  self-coupling  $\lambda_{hH^+H^-}$ , along with the modified Higgs/fermion and Higgs/gauge boson interactions, are responsible for a highly characteristic phenomenological pattern. To illustrate it, we shall concentrate on the following quantities: i) the total (unpolarized and averaged) cross-section  $\langle\sigma_{\gamma\gamma\rightarrow h}\rangle(s)$ , which results from the convolution of the “hard” scattering cross-section  $\hat{\sigma}(\gamma\gamma \rightarrow h)$  with the photon luminosity distribution (describing the effective  $e^\pm \rightarrow \gamma$  conversion of the primary linac beam). For the latter we use the parametrization included in the standard package CompAZ [28]); ii) the relative strength  $r$  of the effective  $\gamma\gamma h$  interaction normalized to the SM (upon identifying  $M_{H_{\text{SM}}}$  with  $M_{h^0}$ ), namely  $r \equiv g_{\gamma\gamma h}/g_{\gamma\gamma H}^{\text{SM}}$ , by which we aim at quantifying the departure of the genuine dynamical features of the 2HDM with respect to the SM.

The results of our numerical analysis of  $r$  are displayed in fig. 4. A first observation is that, unsurprisingly, the profile of  $g_{\gamma\gamma h^0}$  is mainly modulated by the strength of the  $3h$  coupling  $\lambda_{h^0 H^+ H^-}$ . This is a consequence of a destructive interference between the contributions from the loop diagrams triggered by the Higgs boson self-interactions  $h^0 H^+ H^-$  and those induced on the one hand by the gauge bosons and those driven by the Yukawa interactions with neutral Higgs bosons and fermions on the other (cf. fig. 2 of [10]). The impact of such interference is well visible for wide areas of the parameter

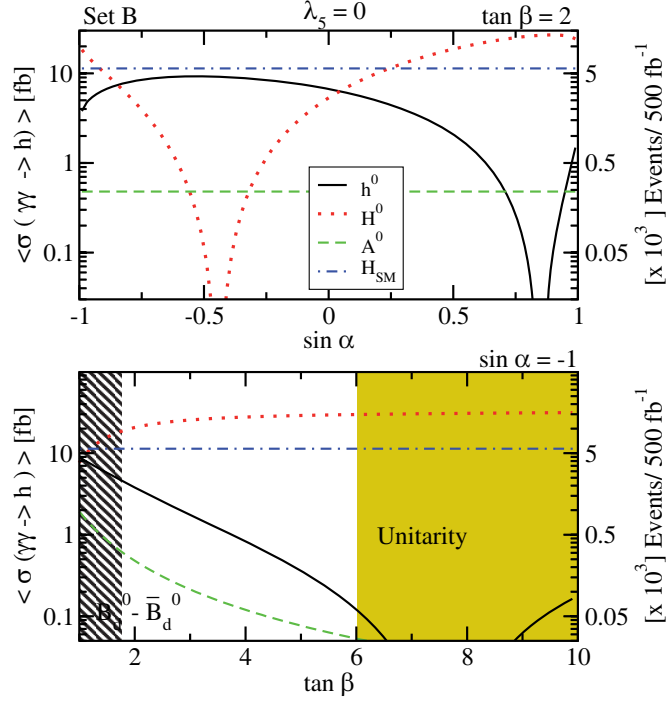


Fig. 5. – (Colour on-line) Averaged cross-section  $\langle \sigma_{\gamma\gamma \rightarrow h} \rangle (\sqrt{s} = 500 \text{ GeV})$  (in fb) as a function of  $\tan \beta$  (top panel) and  $\sin \alpha$  (bottom panel), for Set B of Higgs boson masses and  $\lambda_5 = 0$ . The yellow-shaded (respectively, orange-dashed) areas are disallowed by unitarity (respectively,  $\bar{B}_d^0 - B_d^0$ ) constraints.

space where the strong departures from  $r \simeq 1$  can be traded to suppressions of order 40–60% for the effective  $g_{\gamma\gamma h}$  interaction as compared to the SM. Away from these depleted domains, maximum cross-sections of order  $\sigma \sim \mathcal{O}(10) \text{ fb}$ —*viz.* up to a few thousand events per  $500 \text{ fb}^{-1}$ —are attainable for both  $h^0$  and  $H^0$  (cf. fig. 5 for the dependence of the cross-section on  $\sin \alpha$  and  $\tan \beta$ ). Interestingly enough, the optimal production rates are nicely complementary for the  $CP$ -even channels  $\gamma\gamma \rightarrow h^0$  and  $\gamma\gamma \rightarrow H^0$ , as a result of the inverse correlation of the respective  $\lambda_{hH^+H^-}$  self-couplings (see table II of [5])—and hence of the dominant interference effects. In contrast, owing to the  $CP$ -odd nature of  $A^0$ , the  $\gamma\gamma A^0$  channel appears to be rather featureless and has a milder numerical impact.

Besides the  $3h$  self-couplings, further 2HDM mechanisms could contribute, at least in principle, to shift the  $r$  ratio from its canonical value  $r = 1$ . For example,  $r > 1$  could be achieved for  $\tan \beta \sim 0.2\text{--}0.3$  (cf. fig. 4) as a result of the enhanced Higgs-top ( $\sim 1/\tan \beta$ ) Yukawa coupling. In practice, however, the  $B_d^0 - \bar{B}_d^0$  bounds exclude this possibility. Significant departures from the SM may arise as well within large  $\lambda_5$  scenarios, such as those analyzed in [10]. This possibility is nonetheless highly disfavored if the unitarity conditions are included in their most restrictive version [19].

All in all, trademark hints of a 2HDM structure may emerge from  $\gamma\gamma \rightarrow h$ , mainly through a missing number of events with respect to the SM predictions—as long as the



overall rates are still large enough to be efficiently discriminated from the dominant background process,  $\gamma\gamma \rightarrow b\bar{b}$ . We have shown that this situation can still be realized in sizeable regions of the parameter space, provided the  $3h$  self-couplings take on moderate values (*viz.*  $\lambda_{3h} \sim \mathcal{O}(10^2)$  GeV) preserving unitarity. In contrast, in the MSSM the genuine supersymmetric (slepton/squark-mediated) contributions to  $g_{\gamma\gamma h}$  can only induce rather tempered quantum effects as compared to the general 2HDM, the main reason being the absence of potentially large  $3h$  self-couplings, and hence the lack of a mechanism able to prompt the characteristic interference pattern that we have identified above. Although alternative enhancing effects on  $\gamma\gamma \rightarrow h$  within the MSSM are possible [29], *e.g.*, through (light) stop-mediated loops with large trilinear ( $A_t$ ) couplings and sizable mass splittings between their chiral components  $\tilde{t}_1, \tilde{t}_2$ , they are nevertheless comparably weaker. In fact, these effects are always pulled down by inverse powers of the SUSY breaking scale and are further limited by the stringent limits on the squark and Higgs boson masses, as well as from  $B$ -meson physics—cf. the recent ref. [30] for a fully updated MSSM analysis and a comparison with the general 2HDM case. The bottom-line is that mild deviations from  $r = 1$  of order  $-5\%$  characterize the typical MSSM scenarios. In this sense, it is worth emphasizing that, even if a pattern of the sort  $r \lesssim 1$  would overlap with the 2HDM predictions for small  $3h$  self-couplings (*viz.*  $\lambda_{3h} \sim 10$  GeV), the correlation of  $\gamma\gamma \rightarrow h^0$  and  $\gamma\gamma \rightarrow H^0$  could still help to disentangle both models. Indeed, in the 2HDM both  $CP$ -even channels could simultaneously yield  $\sigma \sim 1\text{--}10$  fb, whilst such situation is definitely precluded in the MSSM owing to the SUSY restrictions on the Higgs boson mass splittings—see [30] for details.

#### 4. – Discussion and conclusions

In this work, we have described several phenomenological aspects of one-loop Higgs boson production processes within the general 2HDM at the future Linear Colliders. We have revisited our previous results and cast them into a common, fully updated framework, including the most recent set of theoretical and experimental constraints presently available in the literature—most significantly those stemming from unitarity and flavor physics. Our brought-to-date analysis keeps on highlighting the truly instrumental role reserved to the future linac facilities, and also the great degree of complementarity of the  $e^+e^-$  and  $\gamma\gamma$  running modes.

We have provided detailed, quantum-corrected predictions for the exclusive pairwise production of Higgs bosons  $e^+e^- \rightarrow 2h = h^0A^0, H^0A^0$  as well as for the Higgs-strahlung channels  $e^+e^- \rightarrow hZ = h^0Z, H^0Z$  at  $\mathcal{O}(\alpha_{ew}^3)$  and leading  $\mathcal{O}(\alpha_{ew}^4)$ . In the case of  $2h$  production, we have shown that the radiative corrections can reach the level of  $|\delta_r| \sim 50\%$  for enhanced  $3h$  self-couplings—mostly for low  $\tan\beta$  and  $|\lambda_5| \sim \mathcal{O}(10)$ —and hence give rise to a substantial positive boost with respect to the tree-level expectations (around  $\sqrt{s} \simeq 500$  GeV) or suppression (for  $\sqrt{s} > 600$  GeV). In the case of the  $hZ$  final states the quantum effects can be of the same order of magnitude, but they are negative for essentially the whole  $\sqrt{s}$  range. Optimal rates for these processes lie in the ballpark of  $\mathcal{O}(10\text{--}100)$  fb and can be attained for typical Higgs masses in the 100–300 GeV range.

No less crucial is the role of the  $3h$  self-couplings in the production of a single Higgs boson from direct  $\gamma\gamma$  collisions. A trademark suppression of  $\sigma(\gamma\gamma \rightarrow h)$  with respect to the SM predictions is singled out, and its origin traced back to the interference effects between the different one-loop contributions, these being critically modulated by the strength of the  $3h$  self-couplings  $hH^+H^-$ . In regions of the parameter space for which this depletion is moderate (*viz.*  $\lambda_{hH^+H^-} \sim \mathcal{O}(10\text{--}100)$  GeV), still significant cross-sections



up to  $\sigma \sim 10 \text{ fb}$  may be retrieved for both  $h^0$  and  $H^0$ . From the experimental point of view, the opportunities for accessing this kind of final states are deemed to be excellent. The decay signatures of the neutral  $CP$ -even states would essentially boil down to  $h^0 \rightarrow b\bar{b}/\tau^+\tau^-$  or  $h^0 \rightarrow VV \rightarrow 4l, 2l + \cancel{E}_T$ , all of them allowing for a comfortable tagging in the clean linac environment. Interestingly enough, the described phenomenology is particularly distinctive of a non-supersymmetric 2HDM structure. In the MSSM, potential enhancements cannot be triggered by the Higgs self-interactions—which are anchored by the gauge couplings—but instead by the Yukawa interactions of the Higgs bosons and the sfermions. These give rise, in general, to rather tempered quantum effects, as compared to the sizable corrections that are spotlighted for the 2HDM. Likewise, the conditions that SUSY dictates on the Higgs spectrum may be of relevance here. For instance, genuine indication of non-standard, non-SUSY Higgs physics may come from the simultaneous observation of  $\gamma\gamma \rightarrow h^0$  and  $\gamma\gamma \rightarrow H^0$ ; both channels may yield  $\mathcal{O}(10^3)$  events per  $500 \text{ fb}^{-1}$ —a situation which could never be ascribed to the MSSM, as the mass splitting between the two Higgs bosons is enforced to be much larger. Finally, the combined analysis of these signatures together with complementary multi-Higgs production channels (cf. ref. [5]) could unveil a characteristic pattern of signatures for different values of  $\sqrt{s}$ . If confirmed, it would point to a non-standard, non-supersymmetric origin. Conversely, if the two  $CP$ -even states would be produced at measurable rates differing by, say, one order of magnitude, this could be compatible with MSSM Higgs physics (see [30] for details), but it would require a detailed dijet invariant mass reconstruction to resolve the spectrum and check if it is compatible with the MSSM constraints.

\* \* \*

JS would like to thank the organizers of the LC 2010 workshop at the INFN-Laboratori Nazionali di Frascati for the kind invitation to present this review. This work has been supported in part by DIUE/CUR Generalitat de Catalunya under project 2009SGR502; by MEC and FEDER under project FPA2010-20807, and by the Spanish Consolider-Ingénio 2010 program CPAN CSD2007-00042.

## REFERENCES

- [1] HABER H., *J. Phys. Conf. Ser. G*, **259** (2010) 012017, arXiv:1011.1038.
- [2] *ILC Reference Design Report Volume 2: Physics at the ILC*, arXiv:0709.1893; WEIGLEIN G. *et al.*, *Physics interplay of the LHC and the ILC.*, *Phys. Rep.*, **426** (2006) 47, hep-ph/0410364.
- [3] GUNION J. F., HABER H. E., KANE G. L. and DAWSON S., *The Higgs hunter's guide* (Addison-Wesley, Menlo-Park) 1990; BRANCO G. C., FERREIRA P. M., LAVOURA L., REBELO M. N., SHER M. and SILVA J. P., *Theory and phenomenology of two-Higgs-doublet models*, arXiv:1106.0034.
- [4] NILLES H. P., *Phys. Rep.*, **110** (1984) 1; HABER H. E. and KANE G. L., *Phys. Rep.*, **117** (1985) 75; FERRARA S. (Editor), *Supersymmetry*, Vol. **1-2** (North Holland, World Scientific) 1987.
- [5] LÓPEZ-VAL D. and SOLÀ J., *Phys. Rev. D*, **81** (2010) 033003, arXiv:0908.2898; *Fortsch. Phys. G*, **58** (2010) 660; PoS RADCOR2009, 045 (2010), arXiv:1001.0473.
- [6] COARASA J. A., GARCIA D., GUASCH J., JIMÉNEZ R. A. and SOLÀ J., *Eur. Phys. J C*, **2** (1998) 373, hep-ph/9607485; *Phys. Lett. B*, **425** (1998) 329, hep-ph/9711472; COARASA J. A., GUASCH J., SOLÀ J. and HOLLIK W., *Phys. Lett. B*, **442** (1998) 326, hep-ph/9808278; GARCIA D., HOLLIK W., JIMÉNEZ R. A. and SOLÀ J., *Nucl. Phys. B*, **427** (1994) 53, hep-ph/9402341; BÉJAR S., GUASCH J., LÓPEZ-VAL D. and SOLÀ J., *Phys. Lett. B*, **668** (2008) 364, arXiv:0805.0973.

- [7] FERRERA G., GUASCH J., LÓPEZ-VAL D. and SOLÀ J., *Phys. Lett. B*, **659** (2008) 297; PoS RADCOR2007, 043 (2007), arXiv:0801.3907.
- [8] HODGKINSON R. N., LÓPEZ-VAL D. and SOLÀ J., *Phys. Lett. B*, **673** (2009) 47, arXiv:0901.2257.
- [9] ARHRIB A., BENBRIK R. and CHIANG C.-W., *Phys. Rev. D*, **77** (2008) 115013, arXiv:0802.0319.
- [10] BERNAL N., LÓPEZ-VAL D. and SOLÀ J., *Phys. Lett. B*, **677** (2009) 39, arXiv:0903.4978.
- [11] CORNET F. and HOLLIK W., *Phys. Lett. B*, **669** (2008) 58; ASAKAWA E., HARADA D., KANEMURA S., OKADA Y. and TSUMURA K., *Phys. Lett. B*, **672** (2009) 354; ARHRIB A., BENBRIK R., CHEN C.-H. and SANTOS R., *Phys. Rev. D*, **80** (2009) 015010; ASAKAWA E., HARADA D., KANEMURA S., OKADA Y. and TSUMURA K., *Phys. Rev. D*, **82** (2010) 115002.
- [12] POSCH P., *Phys. Lett. B*, **696** (2011) 447; PHALEN D., THOMAS B. and WELLS J. D., *Phys. Rev. D*, **75** (2007) 117702; ARHRIB A., HOLLIK W., PEÑARANDA S. and PEYRANÈRE M. CAPDEQUI, *Phys. Lett. B*, **579** (2004) 361; GINZBURG I. F., KRAWCZYK M. and OSLAND P., *Nucl. Instrum. Methods A*, **472** (2001) 149.
- [13] ARHRIB A. and MOULTAKA G., *Nucl. Phys. B*, **558** (1999) 3; ARHRIB A., PEYRANÈRE M. CAPDEQUI, HOLLIK W., MOULTAKA G., *Nucl. Phys. B*, **581** (2000) 34; GUASCH J., HOLLIK W. and KRAFT A., *Nucl. Phys. B*, **596** (2001) 66.
- [14] LÓPEZ-VAL D., SOLÀ J. and BERNAL N., *Phys. Rev. D*, **81** (2010) 113005, arXiv:1003.4312.
- [15] CHANKOWSKI P., POKORSKI S. and ROSIEK J., *Nucl. Phys. B*, **423** (1994) 437; DRIESEN V. and HOLLIK W., *Z. Phys. C*, **68** (1995) 485; DJOUADI A., HABER H. E. and ZERWAS P. M., *Phys. Lett. B*, **375** (2003) 1996; DRIESEN V., HOLLIK W. and ROSIEK J., *Z. Phys. C*, **71** (1996) 259; DJOUADI A., KILIAN W., MÜHLEITNER M. and ZERWAS P. M., *Eur. Phys. J C*, **10** (1999) 27; HEINEMEYER S., HOLLIK W., ROSIEK J. and WEIGLEIN G., *Int. J. Mod. Phys.*, **19** (2001) 535; LOGAN H. E. and SU S.-F., *Phys. Rev. D*, **66** (2003) 035001; CONIAVITIS E. and FERRARI A., *Phys. Rev. D*, **75** (2007) 015004; BREIN O. and HAHN T., *Eur. Phys. J. C*, **52** (2007) 397.
- [16] MORETTI M., PICCININI F., PITTAU R. and RATHSMAN J., *JHEP*, **11** (2010) 097; AOKI M. *et al.*, arXiv:1104.3178; BHATTACHARYYA G., LESER P. and PAS H., *Phys. Rev. D*, **83** (2011) 011701.
- [17] EL KAFFAS A. WAHAB, OSLAND P. and GREID O. M., *Phys. Rev. D*, **76** (2007) 095001; FLÄCHER H., GOEBEL M., HALLER J., HÖCKER A., MÖNIG K. and STELZER J., *Eur. Phys. J. C*, **60** (2009) 543; MAHMOUDI N. and STAL O., *Phys. Rev. D*, **81** (2010) 035016.
- [18] MAHMOUDI F., <http://superiso.in2p3.fr>; *Comput. Phys. Commun.*, **178** (2008) 745, arXiv:0710.2067; **180** (2009) 1579, arXiv:0808.3144.
- [19] KANEMURA S., KUBOTA T. and TAKASUGI E., *Phys. Lett. B*, **313** (1993) 155; AKEROYD A. G., ARHRIB A. and NAIMI E.-M., *Phys. Lett. B*, **490** (2000) 119. See also sect. III of ref. [5].
- [20] SHER M., *Phys. Rep.*, **179** (1989) 273; NIE S. and SHER M., *Phys. Lett. B*, **449** (1999) 89; KANEMURA S., KASAI T. and OKADA Y., *Phys. Lett. B*, **471** (1999) 182; FERREIRA P. M. and JONES D. R. T., *JHEP*, **08** (2009) 069.
- [21] BOHM M., SPIESBERGER H. and HOLLIK W., *Fortsch. Phys. G*, **34** (1986) 87; DENNER A., *Fortsch. Phys. G*, **41** (1993) 307.
- [22] ERIKSSON D., RATHSMAN J. and STAL O., *Comput. Phys. Commun. G*, **181** (2010) 189, arXiv:0902.0851, <http://www.isv.uu.se/thepp/MC/2HDMC/>.
- [23] BECHTLE P., BREIN O., HEINEMEYER S., WEIGLEIN G. and WILLIAMS K. E., *Comput. Phys. Commun. G*, **181** (2010) 138; arXiv:1102.1898, <http://www.ippp.dur.ac.uk/HiggsBounds>.
- [24] HAHN T., *FeynArts 3.2*, *FormCalc* and *LoopTools* user's guides, available from <http://www.feynarts.de>; HAHN T., *Comput. Phys. Commun.*, **168** (2005) 78.
- [25] BJORKEN J. D., in *Proceedings of the 1976 SLAC Summer Inst. on Particle Phys.*, edited by ZIPF M. (SLAC Rep. No. 198, 1976), p. 22; JONES D. R. T. and PETCOV S. T., *Phys. Lett. B*, **84** (1979) 440.

- [26] See *e.g.* TELNOV V. I., *Nucl. Phys. Proc. Supp.*, **184** (2008) 271; *Acta Phys. Pol. B*, **37** (2006) 1049; DE ROECK A., *Nucl. Phys. Proc. Supp.*, **179-180** (2008) 94; BADELEK B. *et al.*, *Int. J. Mod. Phys. A*, **19** (2004) 5097.
- [27] ELLIS J., GAILLARD M. K. and NANOPOULOS D. V., *Nucl. Phys. B*, **106** (1976) 292.
- [28] TELNOV V. I., *Acta Phys. Pol. B*, **37** (2006) 633; ZARNECKI A. F., *Acta Phys. Pol. B*, **34** (2003) 2741.
- [29] GRZADKOWSKI B., GUNION J. F., *Phys. Lett. B*, **294** (1992) 361; GUNION J. F. and HABER H. E., *Phys. Rev. D*, **48** (1993) 5; BORDEN D. L., BAUER D. A. and CALDWELL D. O., *Phys. Rev. D*, **48** (1993) 4018; ZHU S.-H., LI C.-S. and GAO C.-S., *Chin. Phys. Lett.*, **15** (1998) 2; MÜHLEITNER M., KRÄMER M., SPIRA M. and ZERWAS P., *Phys. Lett. B*, **508** (2001) 311; ASNER D. M., GRONBERG J. B. and GUNION J. F., *Phys. Rev. D*, **67** (2003) 035009; KRAWCZYK M., hep-ph/0307314; NIEZURAWSKI P., ZARNECKI A. F. and KRAWCZYK M., *Acta Phys. Pol. B*, **37** (2006) 1187.
- [30] LÓPEZ-VAL D. and SOLÀ J., *Single Higgs-boson production at a photon-photon collider: general 2HDM versus MSSM*, arXiv:1106.3226.